

# Analyst

Accepted Manuscript

This article can be cited before page numbers have been issued, to do this please use: S. Xu, A. K. Badu-Tawiah, S. R. Acharya and R. Speidel, *Analyst*, 2026, DOI: 10.1039/D6AN00268D.



This is an Accepted Manuscript, which has been through the Royal Society of Chemistry peer review process and has been accepted for publication.

Accepted Manuscripts are published online shortly after acceptance, before technical editing, formatting and proof reading. Using this free service, authors can make their results available to the community, in citable form, before we publish the edited article. We will replace this Accepted Manuscript with the edited and formatted Advance Article as soon as it is available.

You can find more information about Accepted Manuscripts in the [Information for Authors](#).

Please note that technical editing may introduce minor changes to the text and/or graphics, which may alter content. The journal's standard [Terms & Conditions](#) and the [Ethical guidelines](#) still apply. In no event shall the Royal Society of Chemistry be held responsible for any errors or omissions in this Accepted Manuscript or any consequences arising from the use of any information it contains.

# Differentiation of Disaccharide Isomers via Diagnostic-Ion-Weighted Spectral Library Searching using Data from Tandem MS Analysis of Chloride Adducts

*Shixiang Xu, Santosh R. Acharya, Ruth M. Speidel, and Abraham K. Badu-Tawiah\**

Department of Chemistry and Biochemistry, The Ohio State University, Columbus, OH 43210, USA

\*Correspondence to Dr. Abraham K. Badu-Tawiah

100 W. 18<sup>th</sup> Avenue, Columbus OH, 43210

Email: badu-tawiah.1@osu.edu

Tel.: 614-292-4276

Fax: (614) 292-1685

Analyst Accepted Manuscript

1  
2  
3  
4  
5  
6  
7  
8  
9  
10  
11  
12  
13  
14  
15  
16  
17  
18  
19  
20  
21  
22  
23  
24  
25  
26  
27  
28  
29  
30  
31  
32  
33  
34  
35  
36  
37  
38  
39  
40  
41  
42  
43  
44  
45  
46  
47  
48  
49  
50  
51  
52  
53  
54  
55  
56  
57  
58  
59  
60

Open Access Article. Published on 30 April 2022. Downloaded on 5/1/2022 10:24:52 AM.  
This article is licensed under a Creative Commons Attribution-NonCommercial 3.0 Unported Licence.



**ABSTRACT:** Rare sugars, comprising of over 50 known saccharide isomers, have broad significance in food science, pharmaceuticals, and biomedical applications. However, the inherent structural complexity (due to isomerization) and low natural abundance of these saccharides pose substantial analytical challenge toward their characterization. Herein, we developed a spectral library searching platform capable of distinguishing disaccharide isomers based on chloride-adducted ( $M+Cl^-$ ) tandem MS (MS/MS) data. A set of unique diagnostic fragment ions were generated from each of the 15 disaccharide isomers allowing a spectral similarity algorithm to be developed incorporating diagnostic-ion weighing to improve isomer differentiation. The resulting diagnostic-ion-weighted scores enabled discrimination among stereoisomers, linkage isomers, and compositional isomers. As a direct infusion MS/MS method, we tested spectral library searching for binary mixtures using both a traditional algorithm without diagnostic ion weighing and our method based on diagnostic ion weighing. With our platform incorporating diagnostic ion weighing, false positive assignments were reduced from 74 to 21 and true negatives increased from 555 to 608. Finally, we applied the method to analyze complex mixtures such as apple juice, coca cola, and Rhinegeist beer. In all cases, the known disaccharide isomers were confirmed by our diagnostic-ion-weighted library searching workflow. Collectively, these results suggest that negative-ion MS/MS data derived from conventional collision-induced dissociation can be a powerful method for saccharide isomer characterization especially when paired with automated spectral library searching algorithms.

**KEYWORDS:** Rare sugars; Chloride adduction; mass spectrometry; Isomer differentiation; Spectral library searching.

1  
2  
3  
4  
5  
6  
7  
8  
9  
10  
11  
12  
13  
14  
15  
16  
17  
18  
19  
20  
21  
22  
23  
24  
25  
26  
27  
28  
29  
30  
31  
32  
33  
34  
35  
36  
37  
38  
39  
40  
41  
42  
43  
44  
45  
46  
47  
48  
49  
50  
51  
52  
53  
54  
55  
56  
57  
58  
59  
60

Open Access Article. Published on 20 April 2016. Downloaded on 5/1/2016 10:24:52 AM.  
This article is licensed under a Creative Commons Attribution-NonCommercial 3.0 Unported Licence.



## INTRODUCTION

The current study aims to introduce an improved similarity scoring algorithm based on direct infusion tandem MS (**MS/MS**) analysis of disaccharide isomers ionized through chloride ( $\text{Cl}^-$ ) adduction in the negative-ion mode. The improvement is observed because negative-ion mode MS/MS analyses of the selected rare sugars generated a set of diagnostic fragment ions, which are included in the algorithm in the form of diagnostic-ion weighted computational strategy resulting in superior prediction. The significance of the study is related to the fact that rare sugars, typically composed of low-abundant monosaccharides and their derivatives, have attracted increased attention due to their distinct structures and enhanced biological functions.<sup>1-3</sup> With reduced sweetness and digestion, many rare sugars have proved to be promising alternatives to conventional sugars (e.g., sucrose), with demonstrated benefits in mitigating obesity, Type-2 diabetes, cardiovascular disease, and dental decay.<sup>4-7</sup> Although naturally present in low abundance, the use of industrial enzymatic and microbial processes have greatly reduced the production cost of rare sugars, making them more accessible for research and for application in food and medicine.<sup>2,8</sup> The purpose of the current study is to develop a direct infusion MS method that can be used to effectively characterize small quantities of target rare sugars, especially during the initial synthetic method development where it might not be necessary to prepare milligram scale of material for structure confirmation.

Despite the growing evidence demonstrating rare sugars to be important in human health, accurate characterization of individual rare sugars remains challenging. For example, disaccharide rare sugars are isomers of sucrose differing only in linkage positions and stereochemical arrangements.<sup>8,9</sup> Conventionally, nuclear magnetic resonance (**NMR**) has been used to distinguish such isomers,<sup>10,11</sup> but NMR requires high sample purity in large quantities and prolong data



acquisition times, making it less compatible with high-throughput analysis required for systematic synthesis of the rare sugars. Spectroscopic techniques such as infrared and ultra violet-visible spectroscopy are rapid but generally lack the resolution and sensitivity needed for carbohydrate isomer differentiation.<sup>12</sup> In contrast, mass spectrometry (MS) offers high sensitivity, minimal sample preparation, and strong tolerance for complex mixtures. Nevertheless, MS alone often fails to resolve saccharide isomers due to identical precursor masses. Front-end separation techniques, such as high-performance liquid chromatography (HPLC), capillary electrophoresis and ion mobility spectrometry can aid identification, but they also increase analytical complexity in terms of instrumentation requirements.<sup>13–18</sup> Gas-phase ion activation strategies, especially collision-induced dissociation (CID), are widely employed for isomer differentiation and are a standard feature on most MS platforms.<sup>19,20</sup> However, CID MS/MS is typically based on positive-ion mode analysis of sodium adducts, which yields a limited set of fragments, providing incomplete structural information for isomer differentiation.<sup>21–23</sup>

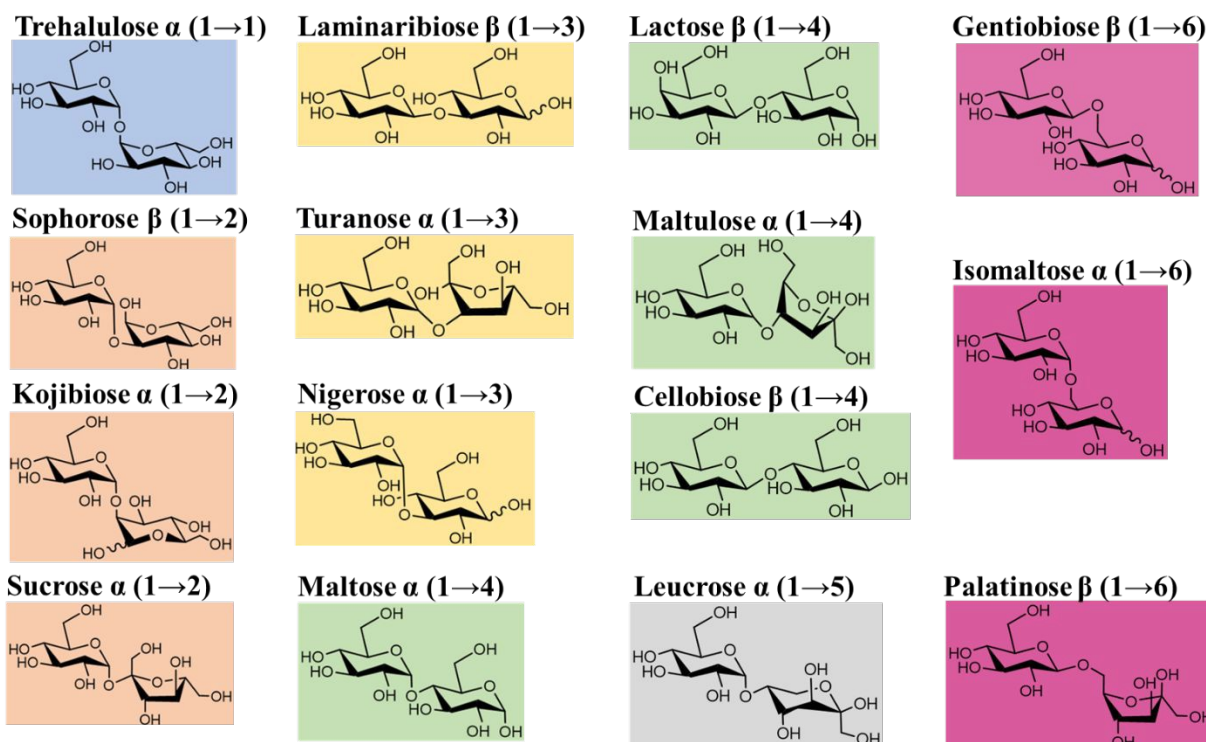


**Figure 1.** Chemical structures of disaccharide isomers studied, which included compositional, linkage, and configurational isomers. The molecular weight of disaccharide isomers is 342 Da.

Unlike positive-ion mode sodium adducts, negative-ion mode analysis of halide adducts of disaccharides has been shown to generate more abundant fragment ions, based on both glycosidic and crossed-ring cleavages, yielding more detailed MS/MS spectra.<sup>24–29</sup> Previous reports demonstrated that chloride adducts  $[M+Cl]^-$  generated by direct-infusion nano-electrospray ionization (**nESI**) produced diagnostic fragment ions under CID MS/MS allowing the differentiation of five rare sugars, which were structural isomers of sucrose, without front-end separation.<sup>3</sup> This finding motivated the development of a spectral library searching approach,<sup>30</sup> which integrates the full MS/MS spectral features with diagnostic fragment ions derived from chloride adducts of disaccharides. The library searching platform automatically identifies the disaccharide isomer, reducing challenges associated with manual interpretation.<sup>31–34</sup> The in-house spectral library was constructed using MS/MS spectra of fifteen (15) closely related disaccharide standards (**Figure 1**) analyzed as chloride adducts  $[M+Cl]^-$  in the negative-ion mode. These disaccharides were selected to represent a broad range of linkage, positional, and stereo/configurational isomers, providing extensive structural diversity for evaluating the accuracy and predictive power of our method. Within this framework, based on spectral library identification, we have developed a normalized dot-product scoring algorithm that integrates MS/MS spectral similarity while applying weights to targeted diagnostic fragment ions to enhance disaccharide characterization.<sup>35–38</sup> Cosine similarity scoring algorithms have been applied in mass spectral library searching, however, most of the published works focused on MS/MS data derived from positive-ion mode analysis of either sodium adducts or protonated species.<sup>31,39</sup> The use of MS/MS data derived from negative-ion mode analysis of chlorides adducts to create mass spectral

1  
2  
3  
4  
5  
6  
7  
8  
9  
10  
11  
12  
13  
14  
15  
16  
17  
18  
19  
20  
21  
22  
23  
24  
25  
26  
27  
28  
29  
30  
31  
32  
33  
34  
35  
36  
37  
38  
39  
40  
41  
42  
43  
44  
45  
46  
47  
48  
49  
50  
51  
52  
53  
54  
55  
56  
57  
58  
59  
60

Open Access Article. Published on 30 April 2022. Downloaded on 5/1/2024 10:24:52 AM.  
This article is licensed under a Creative Commons Attribution-NonCommercial 3.0 Unported Licence.



1  
2  
3 library searching is novel. Additionally, although our previous publication identified diagnostic  
4 fragment ions isomer characterizations were done manually and based on only a single diagnostic  
5 ion. With increased number of isomers (i.e., 15 disaccharide isomers in this study), a single  
6 diagnostic ion was insufficient for isomer differentiation. Therefore, we had to identify new set of  
7 diagnostic ions that collectively form the distinguishing feature of a specific disaccharide isomer.  
8 Therefore, the cosine similarity scoring algorithm described here allowed automatic isomer  
9 identification by evaluating the entire MS/MS spectrum, incorporating specific values of mass-to-  
10 charge ( $m/z$ ) ratio and their relative intensities into the similarity calculation.

11  
12 To validate the platform, we analyzed standard disaccharides in pure form and in binary  
13 mixtures using direct infusion nESI MS/MS. In each case, the workflow demonstrated high  
14 selectivity and accuracy in saccharide isomer identification. Further, the method was applied to  
15 analyze disaccharides in complex matrices including apple extract, beer, and Coca Cola samples.  
16 These samples contain known but diverse carbohydrate composition with multiple disaccharide  
17 isomers, providing an effective means to evaluate the selectivity, sensitivity, and robustness of the  
18 method. Moreover, the spectral library can be continuously expanded with additional saccharide  
19 standards, enhancing its scalability and utility for future studies.<sup>39</sup>  
20  
21  
22  
23  
24  
25  
26  
27  
28  
29  
30  
31  
32  
33  
34  
35  
36  
37  
38  
39  
40  
41  
42  
43  
44  
45  
46  
47  
48  
49  
50  
51  
52  
53  
54  
55  
56  
57  
58  
59  
60



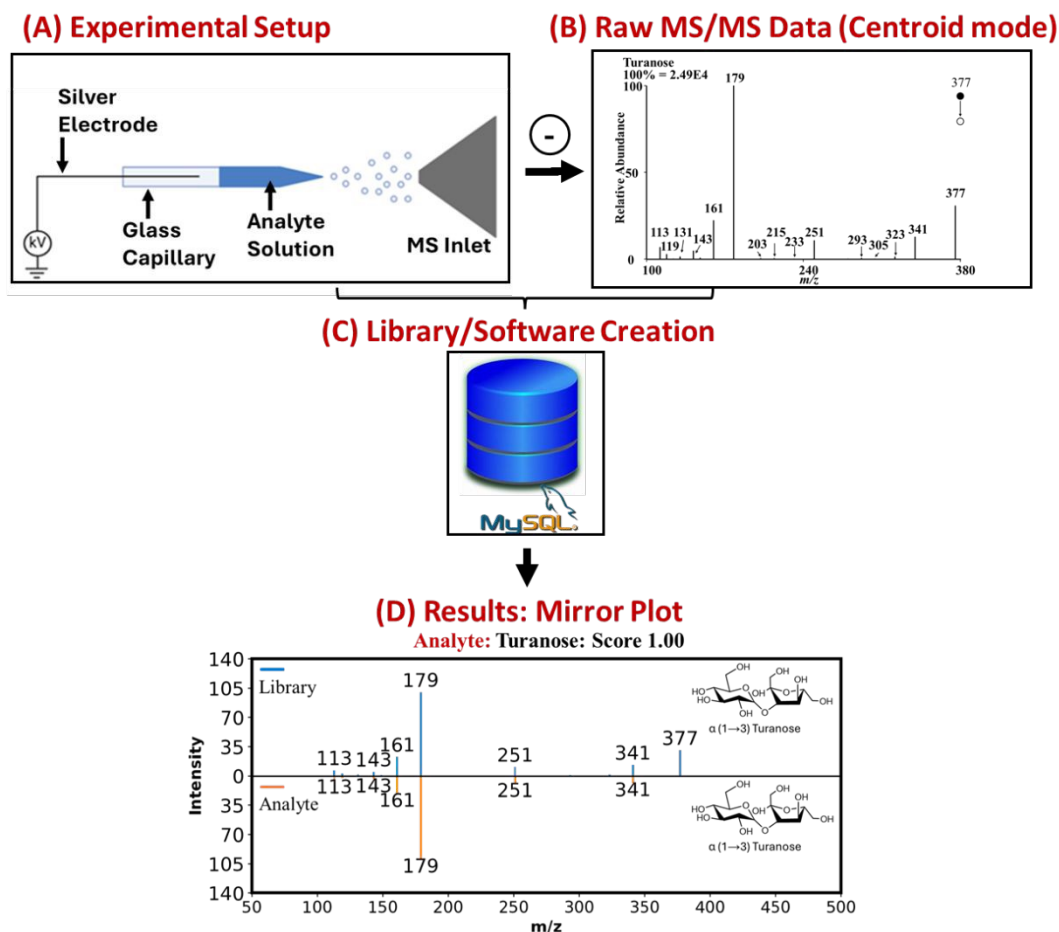


**Figure 2.** Workflow of disaccharide identification based on (A) direct infusion nESI MS/MS analysis using -1.5 kV spray voltage, with (B) MS/MS data recorded in centroid mode. (C) MS/MS spectra were stored using MySQL platform with the search algorithm written using Python. (D) Mirror plot illustrating the output of the library searching.

## EXPERIMENTAL SECTION

**Library and Software Development.** Each MS/MS data file was originally acquired in Thermo Fisher's Xcalibur 2.2 SP1 software, raw format using a Velos Pro ion trap mass spectrometer. The data were subsequently converted to mzML format using MZmine.<sup>40</sup> The mzML file contained 54 scans collected over one minute, with each scan containing a mass-to-charge ( $m/z$ ) array and its corresponding signal intensity. The average  $m/z$  array and signal intensity across all scans were computed to generate a representative dataset, which was subsequently

1  
2  
3  
4  
5  
6  
7  
8  
9  
10  
11  
12  
13  
14  
15  
16  
17  
18  
19  
20  
21  
22  
23  
24  
25  
26  
27  
28  
29  
30  
31  
32  
33  
34  
35  
36  
37  
38  
39  
40  
41  
42  
43  
44  
45  
46  
47  
48  
49  
50  
51  
52  
53  
54  
55  
56  
57  
58  
59  
60

uploaded to MySQL (version 8.0.43) platform. The MySQL library also included annotated diagnostic fragment ion information for each disaccharide isomer (**Figure S1**). An in-house python code was established to compare the MS/MS spectra from the unknown sample against reference spectra stored in the MySQL database. The detailed code can be found in the GitHub repository (<https://github.com/firstvx/Improved-Disaccharide-Isomer-Discrimination-via-Diagnostic-Ion-Weighted-Cl--Adduct-MS-MS/tree/main>). This workflow utilized a spectra similarity algorithm to generate numerical score values and produced mirror plots for compound annotations. A schematic overview of the entire workflow is presented in **Figure 2**.

$$Score = \left( \frac{A \cdot B}{\|A\| \cdot \|B\|} \right) (1 + q) = \left( \frac{\sum_i a_i \cdot b_i}{\sqrt{\sum_i a_i^2} \sqrt{\sum_i b_i^2}} \right) (1 + q) \quad \text{Eqn. (1)}$$

$$\left\{ \begin{array}{l} q = 0.1 \quad \text{Diagnostic ion match for top 28 most intense ions} \\ q = -0.3 \quad \text{No diagnostic ion match for top 28 most intense ions} \end{array} \right.$$

**Equation 1.** Dot-product scoring algorithm integrating MS/MS spectral similarity with targeted diagnostic ions. **A** represents the library spectrum, whereas **B** represents the experimental spectrum.  $a_i$  and  $b_i$  denote the normalized intensities of fragment ion  $m/z_i$  in the experimental and library spectra, respectively.

The numerical value is calculated based on dot-product scoring algorithm that integrates MS/MS spectral similarity while applying weights to targeted diagnostic ions (**Equation 1**).<sup>35–38</sup> Spectra that closely match library references and contain high-intensity diagnostic ions received elevated diagnostic-ion-weighted ( $S_D$ ) scores, whereas spectra with poor matches or missing diagnostic ions yielded lower scores. This approach effectively addresses isomers that generate nearly indistinguishable fragmentation patterns but display subtle variations in relative ion intensities. The  $S_D$  algorithm quantifies spectral similarity on a normalized scale from 0 to 1, where

1  
2  
3 a value of 0 indicates orthogonal (dissimilar) spectra and 1 indicates perfect alignment.<sup>41–44</sup> Such  
4 scoring provides an interpretable numerical value that improves confidence, reproducibility, and  
5 throughput in saccharide isomer identification.<sup>45</sup>  
6  
7  
8  
9

10 **Noncontact Nano-Electrospray Ionization Setup.** For each disaccharide, a 10 mM stock  
11 solution was prepared by dissolving 34.23 mg of the analyte in Milli-Q water. Then, 40  $\mu$ M  
12 working solutions were prepared by appropriate dilution. For  $\text{NH}_4\text{Cl}$ , we first prepared a stock  
13 solution at 1.0 M in water, which was subsequently diluted to 2 mM for analytical use. The final  
14 disaccharide samples were prepared at a concentration of 20  $\mu$ M with 1 mM  $\text{NH}_4\text{Cl}$  in water by  
15 mixing equal volumes of 40  $\mu$ M disaccharide working solution and the 2 mM  $\text{NH}_4\text{Cl}$  solution. For  
16 nano-electrospray ionization (nESI) MS analysis (**Figure 2A**), 10  $\mu$ L of the sample was loaded  
17 into a pulled glass capillary, created in-house from a disposable borosilicate glass (I.D. 1.17 mm;  
18 O.D. 1.5 mm) using a micropipette puller (Model P-97, Sutter Instrument Co., Novato, CA, USA).  
19 The ionization process occurred via non-contact nESI method, which eliminated physical contact  
20 of nESI metal (Ag) electrode with the analyte solution. The non-contact nESI approach reduced  
21 potential analyte oxidation, joule heating, which can damage the glass tip, and improved analytical  
22 sensitivity.<sup>46,47</sup> A spray voltage of -1.5 kV was applied to the silver electrode to generate charged  
23 nanodroplets via an electrostatic induction mechanism.<sup>48–50</sup> The droplets undergo further solvent  
24 evaporation, assisted by heated inlet capillary with the temperature at 250 °C. The nESI glass  
25 capillary was positioned 5 mm in front of the mass spectrometer inlet. The charged nanodroplets  
26 contained the sugar-chloride adducts, which were directly infused into the mass spectrometer for  
27 analysis.  
28  
29  
30  
31  
32  
33  
34  
35  
36  
37  
38  
39  
40  
41  
42  
43  
44  
45  
46  
47  
48  
49  
50

51 **Mass Spectrometry.** All mass spectra were collected using a Thermo Fisher Scientific  
52 Velos Pro ion trap (San Jose, CA, USA). The MS parameters were set as follows based on the  
53  
54  
55  
56  
57  
58  
59  
60

Open Access Article. Published on 30 April 2022. Downloaded on 5/1/2022 10:24:52 AM.  
This article is licensed under a Creative Commons Attribution-NonCommercial 3.0 Unported Licence.



1  
2  
3  
4  
5  
6  
7  
8  
9  
10  
11  
12  
13  
14  
15  
16  
17  
18  
19  
20  
21  
22  
23  
24  
25  
26  
27  
28  
29  
30  
31  
32  
33  
34  
35  
36  
37  
38  
39  
40  
41  
42  
43  
44  
45  
46  
47  
48  
49  
50  
51  
52  
53  
54  
55  
56  
57  
58  
59  
60

previous reported parameters: three microscans, and an ion injection time of 100 ms with data acquired in centroid mode.<sup>3</sup> The precursor ion mass is selected at  $m/z$  377 for chloride adducts in negative-ion mode. The isolation window set at 1.0 with CID setting at collision energy of 30% according to the manufacture's unit. Helium was used as the collisional gas for CID. All data were processed and analyzed by using the Xcalibur 2.2 SP1 software (Thermo Fisher Scientific).

**Chemicals and Reagents.** Sucrose ( $\geq 99.5\%$ ), turanose ( $\geq 98\%$ ), maltulose ( $\geq 99.3\%$ ), nigerose ( $\geq 90\%$ ), leucrose ( $\geq 98\%$ ), lactose ( $\geq 99\%$ ), laminaribiose ( $\geq 95\%$ ), palatinose ( $\geq 98\%$ ), kojibiose ( $\geq 98\%$ ), and sophorose ( $\geq 98\%$ ) were purchased from Sigma-Aldrich (St. Louis, MO). trehalulose ( $\geq 98\%$ ) was obtained from Biosynth International, Inc (San Diego CA). The maltose ( $\geq 98\%$ ), isomaltose ( $\geq 97\%$ ) and gentiobiose ( $\geq 96\%$ ) were purchased from TCI. Cellobiose ( $\geq 99\%$ ) was purchased from MP Biomedicals. HPLC grade acetonitrile and ammonium chloride are purchased from Acros organics (New Jersey, USA) and Sigma-Aldrich (St. Louis, MO), respectively. All sugar powder and ammonium chloride were dissolved in Milli-Q grade water produced in-house. The sugar reagents were first premixed with ammonium chloride and subsequently diluted to yield a 20  $\mu\text{M}$  concentration of sugar and 1 mM ammonium chloride.

**Sample Preparation.** Apple samples (Royal Gala and Granny Smith) were peeled to remove the outer skin. Approximately 1 g of apple flesh was weighed and homogenized using a mortar and pestle. Ten milliliters of Milli-Q water were added to obtain a 100 mg/mL slurry, which was then transferred to an Eppendorf tube (20 mL) and centrifuged at 3000 rpm for 30 min. Approximately 4 mL of the resulting supernatant was transferred to Microsep™ Advance 3 k MW cutoff Centrifugal Filter (Pall Corp., Ann Arbor, MI) and centrifuged at 3000 rpm for 1 h. The filtrate was collected and diluted to a final concentration of 300  $\mu\text{g}/\text{mL}$  in MilliQ water for analysis.

1  
2  
3 The beer sample (Rhinegeist IPA) was opened and allowed to stand for 1 h for degassing. Four  
4 milliliters of the beer was then transferred to molecular-weight-cutoff filters. The filtrate was  
5 collected and diluted 10-fold prior to analysis. Similar approach was used for Coca-Cola samples  
6 where the filtrate was diluted 2000-fold prior to analysis.  
7  
8  
9  
10

## 11 RESULTS AND DISCUSSION

12 **Tandem MS Analysis of Chloride Adducts in Negative-ion Mode.** In negative-ion  
13 mode, saccharides form adduct with chloride anion ( $\text{Cl}^-$ ) to generate stable chloride-adduct.<sup>51–53</sup>  
14 The characteristic chloride isotope ratio of 3:1 for  $^{35}\text{Cl}$ : $^{37}\text{Cl}$  assisted in identifying the saccharide-  
15 related peak in full MS (**Figure S2**). Meanwhile, when the sugar-chloride adduct is subjected to  
16 CID, distinct sets of fragment ions are observed for each disaccharide isomer. In contrast to sugar-  
17 sodium adducts detected in positive-ion mode, which produced limited number of fragments,  
18 chloride adducts produce cleavages at both glycosidic bonds and cross-ring positions, yielding a  
19 more abundant and diverse set of fragment ions.<sup>3</sup> A schematic illustration of all potential fragment  
20 ions in negative-ion mode ( $\text{Cl}^-$  adduct) MS/MS is shown in **Figure 3** with each isomer following  
21 a unique fragmentation pathway characterized by different combinations of common neutral  
22 losses, including HCl,  $\text{H}_2\text{O}$ ,  $\text{CO}_2$  and  $\text{C}_n\text{H}_{2n}\text{O}_n$ .<sup>3,54</sup>  
23  
24  
25  
26  
27  
28  
29  
30  
31  
32  
33  
34  
35  
36  
37  
38  
39  
40  
41  
42  
43  
44  
45  
46  
47  
48  
49  
50  
51  
52  
53  
54  
55  
56  
57  
58  
59  
60

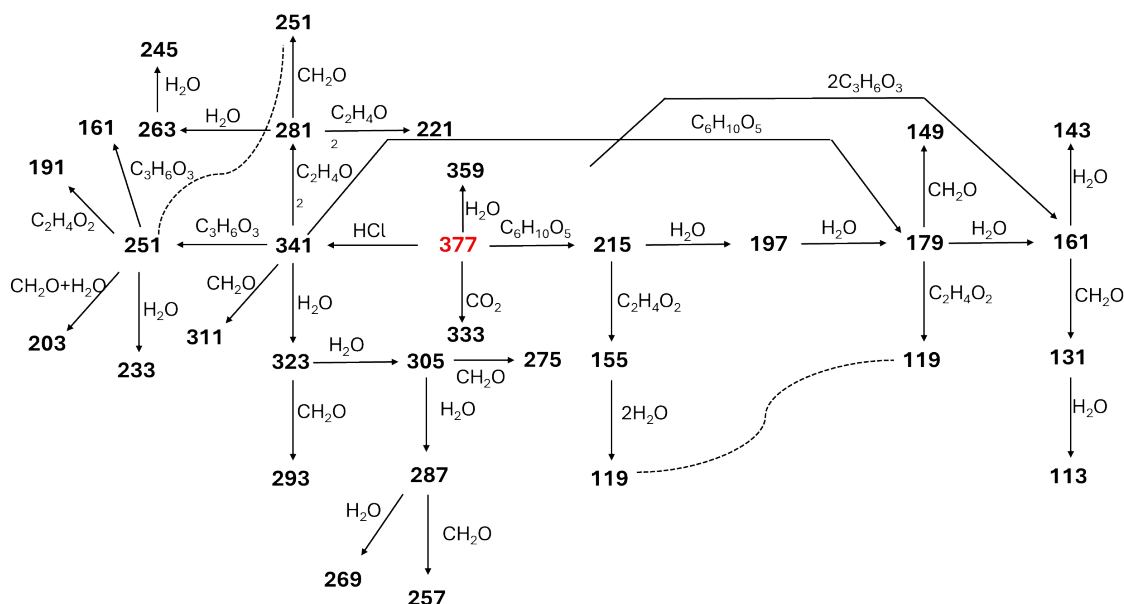


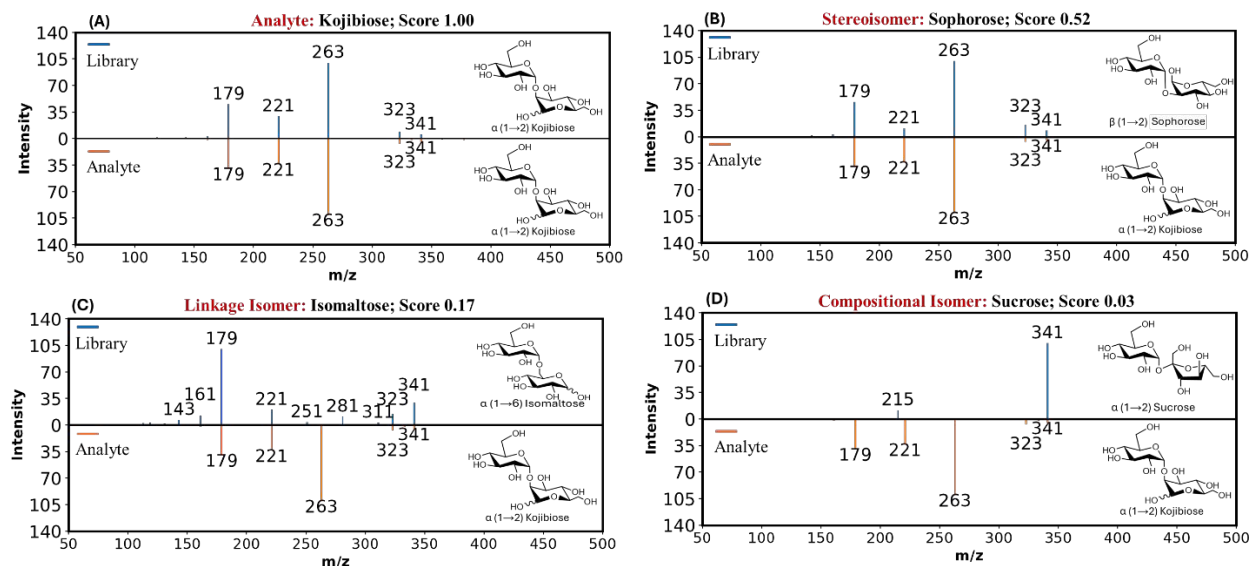
**Figure 3.** Overview of the fragmentation pattern of chloride adducted disaccharides  $[M+Cl]^-$ . All chloride adducted disaccharide isomers were isolated at same precursor mass of  $m/z$  377 with unit isolation width. However, different disaccharide isomers may undergo distinct fragmentation pathway.

The actual MS/MS spectra collected from each of the 15 disaccharide isomers are shown in **Figure S3**, which corroborate the unified fragmentation pathway described in **Figure 3**. In our previous study analyzing five isomers, a single fragment ion was sufficient to serve as a diagnostic ion for differentiating the isomers. However, as the library expanded to 15 disaccharide isomers, reliance on a single diagnostic fragment ion became insufficient for accurate discrimination. Although, in general, isomeric molecules share identical molecular formula and often yield similar fragmentation patterns, differences in peak intensities can still be observed among the 15 disaccharide isomers.<sup>32,55</sup> In the current work, distinct diagnostic fragment ions were established for each disaccharide isomer, selected from the top 28 most intense ions (**Table 1**). The selected diagnostic ions exhibited distinctly higher relative intensity in a given disaccharide compared to other isomers and (2) the specific ion(s) were present in the target isomer and absent (or present at significantly lower intensity) in most other isomers. A candidate isomer that satisfies all selected

diagnostic fragment ions and exhibits strong spectral matching is assigned a higher diagnostic-ion-weighted score; otherwise, the SD score is reduced. These unique sets of fragment ions for each disaccharide provide great distinction between each isomer, which improved isomer characterization compared to utilizing MS/MS spectra only.

**Table 1.** Each disaccharide isomer exhibits a distinct diagnostic ions, with the selected ions falling among the top 28 most intense MS/MS fragment ions.

#	Disaccharide (MW 342 Da)	Diagnostic Fragment Ions from [M+Cl] <sup>-</sup> (Precursor Ion <i>m/z</i> 377)
1	Trehalulose	221/251/269/287/281
2	Sophorose	263/221/359/311/323/245
3	Kojibiose	263/221/359/257/311/323
4	Sucrose	197/215
5	Laminaribiose	191/215/221/233/251
6	Turanose	203/215/233/251/269/293
7	Nigerose	191/215/203/221/233/251
8	Maltose	185/323/221/263/293/275
9	Lactose	115/221/263/293/317/323
10	Maltulose	115/185/221/251/263/293/295
11	Cellobiose	115/215/263/221/245
12	Leucrose	215/233/251/293/311
13	Gentiobiose	221/251/293/311/ 317
14	Isomaltose	221/251/269/293/311/305/317
15	Palatinose	221/251/269/287/293/305/311

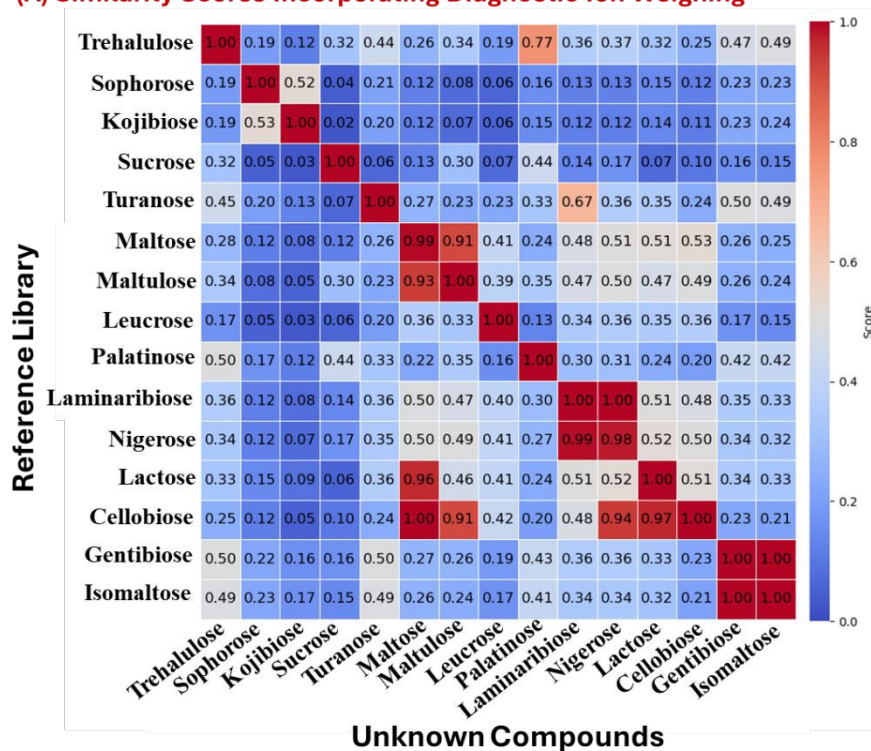
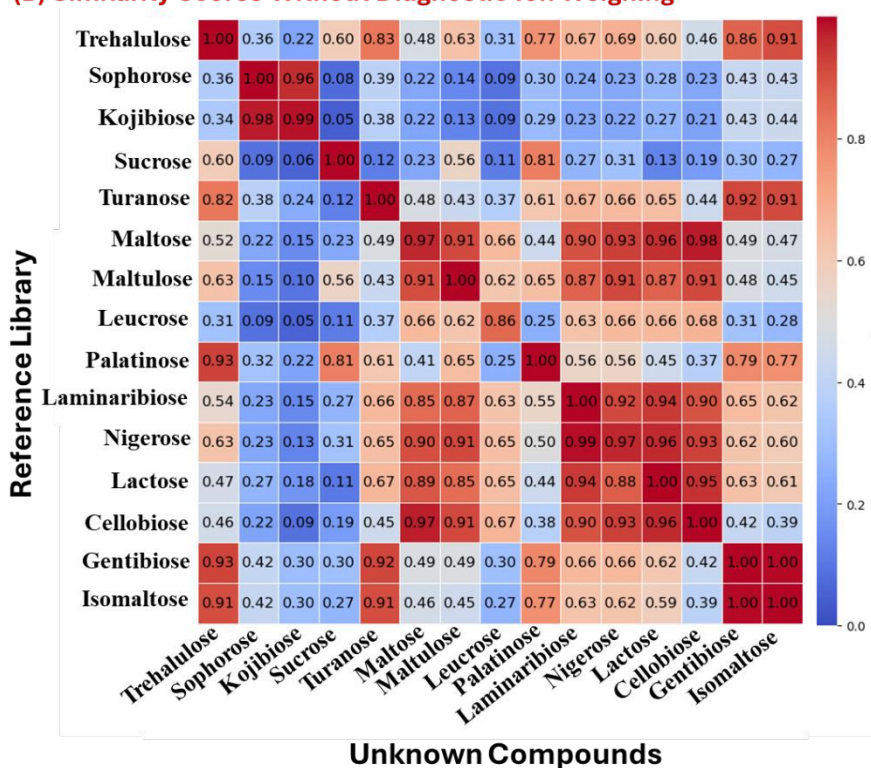


**Figure 4.** MS/MS spectrum of analyte kojibiose is compared with related isomers in the database in the form of mirror plots. (A) Experimental data for kojibiose matches exactly (score 1.0) with previous data stored for kojibiose. Mirror plots comparing experimental data for kojibiose with data previously stored for (B) stereoisomer sophorose, (C) linkage isomer isomaltose, and (D) compositional isomer sucrose, with limited scores of 0.52, 0.17, and 0.03, respectively.

**The Mirror Plot Output.** After constructing the library, which included MS/MS spectra and diagnostic ions for each isomer, we used kojibiose as representative (unknown) analyte to evaluate the performance for the library searching platform. The diagnostic-ion-weighted scores between kojibiose and the other 14 remaining isomers were computed, generating corresponding score value with the mirror plot for visual comparison. **Figure 4** illustrates comparison made for spectrum derived from kojibiose  $\alpha(1\rightarrow2)$  against stereoisomer sophorose  $\beta(1\rightarrow2)$ , linkage isomer isomaltose  $\alpha(1\rightarrow6)$ , and compositional isomer sucrose  $\alpha(1\rightarrow2)$ . As expected, the correct matching isomer [kojibiose  $\alpha(1\rightarrow2)$ ] produced the highest similarity score value 1 (**Figure 4A**), reflecting an excellent match due to the identical fragmentation pattern and the presence of diagnostic ions. The stereo/configurational isomer sophorose  $\beta(1\rightarrow2)$  differ only in the  $\alpha$  and  $\beta$  orientation of the C1 $\rightarrow$ C2 linkage, yet a diagnostic-ion-weighted score of 0.52 (**Figure 4B**) was obtained showing significant differences in the MS/MS data recorded for the two isomers. Likewise, the linkage

1  
2  
3 isomer isomaltose  $\alpha(1\rightarrow6)$  produced even a lower score of 0.17 (**Figure 4C**) indicating high  
4 selectivity between the two isomers. Finally, sucrose  $\alpha(1\rightarrow2)$  which is constitutional isomer  
5 comprising of glucose and fructose rather than the two glucose molecules in kojibiose, produced  
6 much lower score of 0.03 (**Figure 4D**). Collectively, these results highlight the strong isomer  
7 differentiating ability of our platform utilizing the diagnostic-ion-weighted algorithm.  
8  
9  
10  
11  
12  
13  
14  
15  
16  
17  
18  
19  
20  
21  
22  
23  
24  
25  
26  
27  
28  
29  
30  
31  
32  
33  
34  
35  
36  
37  
38  
39  
40  
41  
42  
43  
44  
45  
46  
47  
48  
49  
50  
51  
52  
53  
54  
55  
56  
57  
58  
59  
60



**(A) Similarity Scores Incorporating Diagnostic Ion Weighing****(B) Similarity Scores Without Diagnostic Ion Weighing**

**Figure 5.** Heat maps show similarity scores based on computational algorithm (A) with diagnostic ion weighing and (B) without diagnostic ion weighing.

1  
2  
3  
4  
5  
6  
7  
8  
9  
10  
11  
12  
13  
14  
15  
16  
17  
18  
19  
20  
21  
22  
23  
24  
25  
26  
27  
28  
29  
30  
31  
32  
33  
34  
35  
36  
37  
38  
39  
40  
41  
42  
43  
44  
45  
46  
47  
48  
49  
50  
51  
52  
53  
54  
55  
56  
57  
58  
59  
60

**Two-Dimensional Heat Map Output: Pure Standards.** To emphasize the generality of the observed improved performance for the diagnostic-ion-weighted scoring algorithm, we established a two-dimensional (**2D**) heat map comparing scores with and without the influence of diagnostic fragment ions (**Figure 5**). The heat maps show the comparison between each pure disaccharide standard against the MS/MS spectra stored in the library. In **Figure 5**, the rows represent reference library compounds while the columns represent unknown compounds. Each score was tested with triplicate (independent analysis) measurement to ensure consistency (**Figure S4**). The average score indicates the similarity of MS/MS spectra between unknown and reference spectra. Higher score values (shown in maroon) indicate stronger spectral matches, while blue colors show dissimilarity between unknown sample and reference spectra. The presence of diagonal maroon color patterns along the same rows and columns, corresponding to identical isomeric compounds, demonstrate strong characterization performance. Using a positive decision threshold of approximately 0.9, scores computed with diagnostic ion weighing (**Figure 5A**) achieved clear separation between matching and non-matching isomers with minimal false positives. The 0.9 threshold was empirically established based on observations that consistently yielded true positive identifications, amongst which similarity scores were close to 1.0. Allowing 10% error, the 0.9 threshold enables confident identification. The high performance observed under this condition is due to the integration of overall MS/MS spectral similarity and diagnostic ion weighing. In contrast, when diagnostic fragment ions are excluded (**Figure 5B**), applying the same threshold of 0.9 identifies several true positives but also results in a substantial number of false positive assignments. This comparison underscores the importance of diagnostic ion information, which is available in negative-ion mode with chloride adducted analysis.



As an example of the high selectivity displayed in this work, consider maltose  $\alpha(1\rightarrow4)$ , which is a configurational isomer to cellobiose  $\beta(1\rightarrow4)$ , a linkage isomer to isomaltose  $\alpha(1\rightarrow6)$ , and a compositional isomer to sucrose  $\alpha(1\rightarrow2)$ . In the dot-product analysis without diagnostic ion weighing (**Figure 5B**), the stereo/configurational isomer cellobiose was identified as false positive. Additionally, using threshold score  $>0.90$ , we observed several false positives, including nigerose and lactose. However, the score with diagnostic ion algorithm improved performance by enhancing the score for the correct match while reducing the scores for unmatched isomers, thereby increasing both selectivity and confidence in identification. Again, consider turanose and trehalulose, which produced several false positives (i.e., isomaltose, gentiobiose, and palatinose) when they were characterized using the algorithm without diagnostic ion weighing. These false positive outcomes were eliminated for both analytes when diagnostic ion weighing was employed. Although the diagnostic-ion-weighted algorithm significantly improved disaccharide characterization, certain limitations remain in distinguishing configurational isomers. For example, the score for cellobiose similarity was comparable to scores derived from maltose, lactose, and nigerose (**Figure 5A**). Likewise, gentiobiose and isomaltose were indistinguishable, even with diagnostic ion weighing. After careful consideration, we observed that among the 15 disaccharides tested, several isomers had identical linkage but differed in composition and stereochemistry. These isomers included kojibiose, sophorose, laminaribiose, nigerose, maltose, cellobiose, gentiobiose, and isomaltose. Many of these disaccharides fragmented through a common intermediate (**Figure S5**), resulting in highly similar MS/MS spectra, which posed particular challenge for accurate isomeric differentiation using MS/MS alone. Nonetheless, the results are still relevant because the purpose for developing the direct infusion nESI MS/MS method is to provide opportunities to rapidly characterize minute quantities of isomers synthesized during the

1  
2  
3  
4  
5  
6  
7  
8  
9  
10  
11  
12  
13  
14  
15  
16  
17  
18  
19  
20  
21  
22  
23  
24  
25  
26  
27  
28  
29  
30  
31  
32  
33  
34  
35  
36  
37  
38  
39  
40  
41  
42  
43  
44  
45  
46  
47  
48  
49  
50  
51  
52  
53  
54  
55  
56  
57  
58  
59  
60

Open Access Article. Published on 30 April 2022. Downloaded on 5/1/2022 6:10:24:52 AM.  
This article is licensed under a Creative Commons Attribution-NonCommercial 3.0 Unported Licence.



1  
2  
3 initial stages of the (synthetic) method development. In such circumstances, we expect analytical  
4 sensitivity and speed of analysis to be more important than structural sensitivity since analyte  
5 structure is known.  
6  
7  
8  
9

10 **Two-Dimensional Heat Map Output: Binary Mixture.** The pure standard analysis  
11 yielded promising results for disaccharide characterization. Since most rare sugars are synthesized  
12 from isomerization process, it was necessary to evaluate the ability of the diagnostic-ion-weighted  
13 algorithm to identify the correct isomers in binary mixture systems. We expect such a condition to  
14 exist for incomplete conversion and assuming 100% specificity (e.g., for enzymatic synthetic  
15 method) with no byproducts. Thus, we prepared 53 different binary mixtures by pairing up two  
16 isomers at a time using a set of 12 randomly selected rare and regular sugars: gentiobiose,  
17 isomaltose, kojibiose, lactose, leucrose, maltose, maltulose, palatinose, sophorose, sucrose,  
18 trehalulose, and turanose. The mixtures were analyzed using the non-contact nESI MS/MS  
19 platform and results were subjected to library searching with and without diagnostic ion weighing.  
20 The results of these analyses are summarized in **Figures S6** and **S7**. Here, the scores were  
21 normalized by dividing the maximum score value. Then, four different colors were used to  
22 represent the four potential outcomes of the algorithm: (1) green color for true positive results  
23 (score >0.9), (2) red for false positive results, (3) blue for true negative results, and (4) yellow for  
24 false negative results. That is, green color indicates correctly predicted isomers with diagnostic-  
25 ion-weighted scores exceeding 0.9 threshold (true positives). Red boxes represent incorrectly  
26 predicted isomers with diagnostic-ion-weighted scores exceeding the threshold (false positives).  
27 Yellow corresponds to missed predictions in which a compound should be present, but the  
28 diagnostic-ion-weighted score falls below the threshold (false negatives). Blue color denotes true  
29 negatives, indicating isomers that are correctly identified as absent in the binary mixture.  
30  
31  
32  
33  
34  
35  
36  
37  
38  
39  
40  
41  
42  
43  
44  
45  
46  
47  
48  
49  
50  
51  
52  
53  
54  
55  
56  
57  
58  
59  
60



For example, when the mixture containing trehalulose and sophorose was analyzed, the algorithm with diagnostic ion weighing correctly identified trehalulose to be present (entry #1, **Figure S6**). However, the diagnostic-ion-weighted score of sophorose was not above 0.9, so it was assigned as a false negative prediction. Without diagnostic ion weighing, however, sophorose was correctly identified (entry #1, **Figure S7**). Trehalulose did not show up above score 0.9, indicating false negative results. Besides sophorose, kojibiose also registered a score > 0.9 without diagnostic ion weighing, which resulted in a false positive result. Such false positive is not surprising given that sophorose  $\beta(1\rightarrow2)$  and kojibiose  $\alpha(1\rightarrow2)$  are stereoisomers. No such false positive was observed when the algorithm with diagnostic ion weighing was used. For the analysis of laminaribiose and nigerose mixture (entry #37, **Figure S6**), the two isomers were correctly identified, with no false negative or false positive. When the same MS/MS data was analyzed without diagnostic ion weighing (entry #37, **Figure S7**), five isomers were ranked with scores >0.9. Among the five, laminaribiose and nigerose were correctly identified as true positives, making the remaining three isomers (lactose, maltose, and maltulose) false positive predictions. Among the 53 different binary mixtures analyzed, at least one isomer in the mixture was correctly identified except entry #53 (i.e., isomaltose and palatinose mixture) where both analytes were missed when employing diagnostic ion weighing. Overall, compared to the conventional scoring method, the inclusion of diagnostic ion weighing registered 55 true positives as opposed to 67 for the conventional method. With diagnostic ion weighing, false positive prediction was reduced from 74 to 21 and true negative increase from 555 to 608. Overall, the data show that the scoring method incorporating diagnostic ions significantly improved the performance of isomer characterization in binary mixtures. We expect true positive predictions to improve significantly

1  
2  
3 by employing front-end chromatographic separation, a research direction currently being pursued  
4  
5 in our laboratory.

6  
7  
8 **Analysis of Complex Mixtures.** To evaluate the suitability of the diagnostic-ion-weighted  
9  
10 algorithm toward real-world applications, we analyzed three sample matrices containing known  
11  
12 disaccharides. These samples included Mexican Coca Cola and apple juice, both of which contain  
13  
14 sucrose as the primary disaccharide, as well as Rhinegeist beer, which contains maltose and  
15  
16 lactose.<sup>56,57</sup> After minimal preparation (see experimental section), MS/MS spectra (**Figure S8**)  
17  
18 were recorded from these complex samples using the direct infusion non-contact nESI MS/MS  
19  
20 platform. The spectra were uploaded into the spectral library searching workflow and scores were  
21  
22 computed with and without diagnostic ion weighing. The results from this work are summarized  
23  
24 in **Figure 6** in which the algorithm accurately identified sucrose to be present in both Coca Cola  
25  
26 and apple juice samples, with diagnostic-ion-weighted scores approaching 1.0 (**Figure 6B and C**).  
27  
28 Consistent results were also obtained from the beer sample (**Figure 6A**), where diagnostic-ion-  
29  
30 weighted scores of 1.0, 0.94, and 0.93 were recorded, with spectra matching those stored in our  
31  
32 database for maltose, cellobiose, and lactose, respectively. Although cellobiose is typically not  
33  
34 reported to be present in Rhinegeist beer, its presence has been confirmed in our ongoing HPLC  
35  
36 studies. While the conventional algorithm, without diagnostic ion weighing, correctly predicted  
37  
38 sucrose to be present in both apple juice and Coca Cola, this method failed to identify any of the  
39  
40 disaccharides in the beer sample. Such results reinforce and validate the applicability of the  
41  
42 diagnostic-ion-weighted spectral library searching approach for real-world saccharide isomer  
43  
44 discrimination.  
45  
46  
47  
48  
49  
50  
51  
52  
53  
54  
55  
56  
57  
58  
59  
60



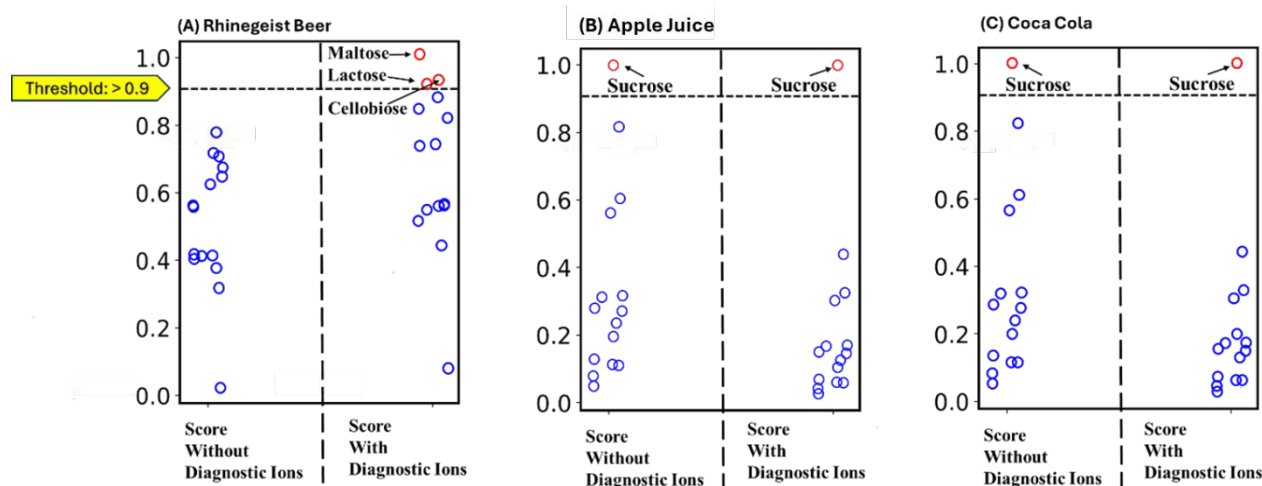


**Figure 6.** Prediction results obtained from our diagnostic-ion-weighted scoring algorithm for disaccharide isomer identification from complex samples: (A) Rhinegeist beer, (B) apple juice, and (C) Coca Cola. Results are compared with computation done without diagnostic ion weighing for each sample. Applying a threshold score on 0.9, maltose, lactose, and cellobiose were identified in Rhinegeist beer sample while only sucrose was identified in both apple juice and Coca Cola.

## CONCLUSION

In conclusion, this study demonstrates a significant improvement in disaccharide isomer characterization. The method is applicable to both rare sugars and common sugars (e.g., sucrose). By incorporating diagnostic fragment ions derived from negative-ion mode chloride adduct MS/MS spectra, the proposed method successfully discriminates among configurational, linkage, and compositional isomers. The library searching framework is robust and allows high-throughput differentiation of isomers. Validation with pure standards showed that correct isomer assignments consistently yielded the highest diagnostic-ion-weighted scores, confirming improved specificity and analytical performance. Similar results were observed for binary mixture analyses, in which the algorithm reduced false positives while maintaining true positives. Finally, application of the platform toward real sample complex mixtures enabled accurate and reproducible identification of disaccharide isomers, demonstrating the reliability, reproducibility, and practical utility of the method in heterogeneous matrices.

## ACKNOWLEDGEMENT

This research was supported by the National Institute of General Medical Sciences under award number R01G130325.

## REFERENCES

- (1) Masuda, Y.; Ohbayashi, K.; Iba, K.; Kitano, R.; Kimura, T.; Yamada, T.; Hira, T.; Yada, T.; Iwasaki, Y. Abilities of Rare Sugar Members to Release Glucagon-like Peptide-1 and Suppress Food Intake in Mice. *Nutrients* **2025**, *17* (7), 1221. <https://doi.org/10.3390/nu17071221>.
- (2) Zhang, W.; Zhang, T.; Jiang, B.; Mu, W. Enzymatic Approaches to Rare Sugar Production. *Biotechnology Advances* **2017**, *35* (2), 267–274. <https://doi.org/10.1016/j.biotechadv.2017.01.004>.
- (3) Amoah, E.; Kulyk, D. S.; Callam, C. S.; Hadad, C. M.; Badu-Tawiah, A. K. Mass Spectrometry Approach for Differentiation of Positional Isomers of Saccharides: Toward Direct Analysis of Rare Sugars. *Anal. Chem.* **2023**, *95* (13), 5635–5642. <https://doi.org/10.1021/acs.analchem.2c05375>.
- (4) Lina, B. A. R.; Jonker, D.; Kozianowski, G. Isomaltulose (Palatinose®): A Review of Biological and Toxicological Studies. *Food and Chemical Toxicology* **2002**, *40* (10), 1375–1381. [https://doi.org/10.1016/S0278-6915\(02\)00105-9](https://doi.org/10.1016/S0278-6915(02)00105-9).
- (5) Elias, P. S.; Benecke, H.; Schwengers, D. Safety Evaluation Studies of Leucrose. *Journal of the American College of Toxicology* **1996**, *15* (3), 205–218. <https://doi.org/10.3109/10915819609008714>.
- (6) Isnard, N.; Péterszegi, G.; Robert, A. M.; Robert, L. Regulation of Elastase-Type Endopeptidase Activity, MMP-2 and MMP-9 Expression and Activation in Human Dermal Fibroblasts by Fucose and a Fucose-Rich Polysaccharide. *Biomedicine & Pharmacotherapy* **2002**, *56* (5), 258–264. [https://doi.org/10.1016/S0753-3322\(02\)00196-8](https://doi.org/10.1016/S0753-3322(02)00196-8).
- (7) Fattahi, M. J.; Abdollahi, M.; Agha Mohammadi, A.; Rastkari, N.; Khorasani, R.; Ahmadi, H.; Tofighi Zavareh, F.; Sedaghat, R.; Tabrizian, N.; Mirshafiey, A. Preclinical Assessment of  $\beta$ -D-Mannuronic Acid (M2000) as a Non-Steroidal Anti-Inflammatory Drug. *Immunopharmacology and Immunotoxicology* **2015**, *37* (6), 535–540. <https://doi.org/10.3109/08923973.2015.1113296>.
- (8) Park, M.-O.; Lee, B.-H.; Lim, E.; Lim, J. Y.; Kim, Y.; Park, C.-S.; Lee, H. G.; Kang, H.-K.; Yoo, S.-H. Enzymatic Process for High-Yield Turanose Production and Its Potential Property as an Adipogenesis Regulator. *J. Agric. Food Chem.* **2016**, *64* (23), 4758–4764. <https://doi.org/10.1021/acs.jafc.5b05849>.
- (9) Gabryelski, W.; Froese, K. L. Rapid and Sensitive Differentiation of Anomers, Linkage, and Position Isomers of Disaccharides Using High-Field Asymmetric Waveform Ion Mobility Spectrometry (FAIMS). *J Am Soc Mass Spectrom* **2003**, *14* (3), 265–277. [https://doi.org/10.1016/S1044-0305\(03\)00002-3](https://doi.org/10.1016/S1044-0305(03)00002-3).
- (10) Sultana, A.; Asghari, A.; Khalloufi, S. A Straightforward Method for Disaccharide Characterization from Transverse Relaxometry Using Low-Field Time-Domain Nuclear

1  
2  
3  
4  
5  
6  
7  
8  
9  
10  
11  
12  
13  
14  
15  
16  
17  
18  
19  
20  
21  
22  
23  
24  
25  
26  
27  
28  
29  
30  
31  
32  
33  
34  
35  
36  
37  
38  
39  
40  
41  
42  
43  
44  
45  
46  
47  
48  
49  
50  
51  
52  
53  
54  
55  
56  
57  
58  
59  
60

Open Access Article. Published on 30 April 2025. Downloaded on 5/1/2025 10:24:52 AM.  
This article is licensed under a Creative Commons Attribution-NonCommercial 3.0 Unported Licence.



- Magnetic Resonance. *Food Anal. Methods* **2024**, *17* (12), 1770–1782.  
<https://doi.org/10.1007/s12161-024-02691-w>.
- (11) Schievano, E.; Tonoli, M.; Rastrelli, F. NMR Quantification of Carbohydrates in Complex Mixtures. A Challenge on Honey. *Anal. Chem.* **2017**, *89* (24), 13405–13414.  
<https://doi.org/10.1021/acs.analchem.7b03656>.
- (12) Kozłowicz, K.; Różyło, R.; Gładyszewska, B.; Matwijczuk, A.; Gładyszewski, G.; Chocyk, D.; Samborska, K.; Piekut, J.; Smolewska, M. Identification of Sugars and Phenolic Compounds in Honey Powders with the Use of GC–MS, FTIR Spectroscopy, and X-Ray Diffraction. *Sci Rep* **2020**, *10* (1), 16269. <https://doi.org/10.1038/s41598-020-73306-7>.
- (13) Butler, K. E.; Kalmar, J. G.; Muddiman, D. C.; Baker, E. S. Utilizing Liquid Chromatography, Ion Mobility Spectrometry, and Mass Spectrometry to Assess INLIGHT™ Derivatized N-Linked Glycans in Biological Samples. *Anal Bioanal Chem* **2022**, *414* (1), 623–637. <https://doi.org/10.1007/s00216-021-03570-7>.
- (14) Matías, J.; González, J.; Royano, L.; Barrena, R. A. Analysis of Sugars by Liquid Chromatography-Mass Spectrometry in Jerusalem Artichoke Tubers for Bioethanol Production Optimization. *Biomass and Bioenergy* **2011**, *35* (5), 2006–2012.  
<https://doi.org/10.1016/j.biombioe.2011.01.056>.
- (15) Pismennõi, D.; Kiritsenko, V.; Marhivka, J.; Kütt, M.-L.; Vilu, R. Development and Optimisation of HILIC-LC-MS Method for Determination of Carbohydrates in Fermentation Samples. *Molecules* **2021**, *26* (12), 3669.  
<https://doi.org/10.3390/molecules26123669>.
- (16) Sluiter, W.; Van Den Bosch, J. C.; Goudriaan, D. A.; Van Gelder, C. M.; De Vries, J. M.; Huijmans, J. G. M.; Reuser, A. J. J.; Van Der Ploeg, A. T.; Ruijter, G. J. G. Rapid Ultrapformance Liquid Chromatography–Tandem Mass Spectrometry Assay for a Characteristic Glycogen-Derived Tetrasaccharide in Pompe Disease and Other Glycogen Storage Diseases. *Clinical Chemistry* **2012**, *58* (7), 1139–1147.  
<https://doi.org/10.1373/clinchem.2011.178319>.
- (17) Liu, Y.; Clemmer, D. E. Characterizing Oligosaccharides Using Injected-Ion Mobility/Mass Spectrometry. *Anal. Chem.* **1997**, *69* (13), 2504–2509. <https://doi.org/10.1021/ac9701344>.
- (18) McKenna, K. R.; Li, L.; Baker, A. G.; Ujma, J.; Krishnamurthy, R.; Liotta, C. L.; Fernández, F. M. Carbohydrate Isomer Resolution via Multi-Site Derivatization Cyclic Ion Mobility-Mass Spectrometry. *Analyst* **2019**, *144* (24), 7220–7226.  
<https://doi.org/10.1039/C9AN01584A>.
- (19) Lee, S.; Valentine, S. J.; Reilly, J. P.; Clemmer, D. E. Analyzing a Mixture of Disaccharides by IMS-VUVPD-MS. *International Journal of Mass Spectrometry* **2012**, *309*, 161–167. <https://doi.org/10.1016/j.ijms.2011.09.013>.
- (20) Zhao, Y.; Kent, S. B. H.; Chait, B. T. Rapid, Sensitive Structure Analysis of Oligosaccharides. *Proc. Natl. Acad. Sci. U.S.A.* **1997**, *94* (5), 1629–1633.  
<https://doi.org/10.1073/pnas.94.5.1629>.
- (21) Nguan, H.-S.; Ni, C.-K. Collision-Induced Dissociation of  $\alpha$ -Isomaltose and  $\alpha$ -Maltose. *J. Phys. Chem. A* **2022**, *126* (47), 8799–8808. <https://doi.org/10.1021/acs.jpca.2c04278>.
- (22) He, H.; Wen, Y.; Guo, Z.; Li, P.; Liu, Z. Efficient Mass Spectrometric Dissection of Glycans via Gold Nanoparticle-Assisted in-Source Cation Adduction Dissociation. *Anal. Chem.* **2019**, *91* (13), 8390–8397. <https://doi.org/10.1021/acs.analchem.9b01217>.
- (23) Fura, Aberra.; Leary, J. A. Differentiation of Calcium(2+)- and Magnesium(2+)-Coordinated Branched Trisaccharide Isomers: An Electrospray Ionization and Tandem

- 1  
2  
3  
4  
5  
6  
7  
8  
9  
10  
11  
12  
13  
14  
15  
16  
17  
18  
19  
20  
21  
22  
23  
24  
25  
26  
27  
28  
29  
30  
31  
32  
33  
34  
35  
36  
37  
38  
39  
40  
41  
42  
43  
44  
45  
46  
47  
48  
49  
50  
51  
52  
53  
54  
55  
56  
57  
58  
59  
60
- Mass Spectrometry Study. *Anal. Chem.* **1993**, *65* (20), 2805–2811.  
<https://doi.org/10.1021/ac00068a017>.
- (24) Harvey, D. J. NEGATIVE ION MASS SPECTROMETRY FOR THE ANALYSIS OF N-LINKED GLYCANS. *Mass Spectrometry Reviews* **2020**, *39* (5–6), 586–679.  
<https://doi.org/10.1002/mas.21622>.
- (25) Chai, W.; Piskarev, V.; Lawson, A. M. Negative-Ion Electrospray Mass Spectrometry of Neutral Underivatized Oligosaccharides. *Anal. Chem.* **2001**, *73* (3), 651–657.  
<https://doi.org/10.1021/ac0010126>.
- (26) Einolf, W. N.; Magin, D. F.; Chan, W. G. Analysis of Carbohydrates by Chemical Ionization Mass Spectrometry. *International Journal of Mass Spectrometry and Ion Physics* **1983**, *48*, 335–338. [https://doi.org/10.1016/0020-7381\(83\)87096-X](https://doi.org/10.1016/0020-7381(83)87096-X).
- (27) Kato, Y.; Numajiri, Y. Chloride Attachment Negative-Ion Mass Spectra of Sugars by Combined Liquid Chromatography and Atmospheric Pressure Chemical Ionization Mass Spectrometry. *Journal of Chromatography B: Biomedical Sciences and Applications* **1991**, *562* (1), 81–97. [https://doi.org/10.1016/0378-4347\(91\)80567-V](https://doi.org/10.1016/0378-4347(91)80567-V).
- (28) Zheng, X.; Zhang, X.; Schocker, N. S.; Renslow, R. S.; Orton, D. J.; Khamsi, J.; Ashmus, R. A.; Almeida, I. C.; Tang, K.; Costello, C. E.; Smith, R. D.; Michael, K.; Baker, E. S. Enhancing Glycan Isomer Separations with Metal Ions and Positive and Negative Polarity Ion Mobility Spectrometry-Mass Spectrometry Analyses. *Anal Bioanal Chem* **2017**, *409* (2), 467–476. <https://doi.org/10.1007/s00216-016-9866-4>.
- (29) Gass, D. T.; Quintero, A. V.; Hatvany, J. B.; Gallagher, E. S. Metal Adduction in Mass Spectrometric Analyses of Carbohydrates and Glycoconjugates. *Mass Spectrometry Reviews* **2024**, *43* (4), 615–659. <https://doi.org/10.1002/mas.21801>.
- (30) DeBono, N. J.; Moh, E. S. X.; Packer, N. H. Experimentally Determined Diagnostic Ions for Identification of Peptide Glycotopes. *J. Proteome Res.* **2024**, *23* (7), 2661–2673.  
<https://doi.org/10.1021/acs.jproteome.3c00858>.
- (31) Geng, F.; Zhou, B.; Yang, P.; Zhang, L.; Zhang, J.; Mao, D.; Guo, Y. Multidimensional Mass Spectral Similarity Algorithm: Discriminate Disaccharide and Flavonoid Isomers Coupled with Online Energy-Resolved Acquisition and Electron Activation Dissociation. *Anal. Chem.* **2025**, *acs.analchem.5c05440*. <https://doi.org/10.1021/acs.analchem.5c05440>.
- (32) Wu, H.-T.; Riggs, D. L.; Lyon, Y. A.; Julian, R. R. Statistical Framework for Identifying Differences in Similar Mass Spectra: Expanding Possibilities for Isomer Identification. *Anal. Chem.* **2023**, *95* (17), 6996–7005. <https://doi.org/10.1021/acs.analchem.3c00495>.
- (33) Xue, J.; Laine, R. A.; Matta, K. L. Enhancing MSn Mass Spectrometry Strategy for Carbohydrate Analysis: A B2 Ion Spectral Library. *Journal of Proteomics* **2015**, *112*, 224–249. <https://doi.org/10.1016/j.jprot.2014.07.013>.
- (34) Ashline, D. J.; Lapadula, A. J.; Liu, Y.-H.; Lin, M.; Grace, M.; Pramanik, B.; Reinhold, V. N. Carbohydrate Structural Isomers Analyzed by Sequential Mass Spectrometry. *Anal. Chem.* **2007**, *79* (10), 3830–3842. <https://doi.org/10.1021/ac062383a>.
- (35) Lam, H.; Deutsch, E. W.; Eddes, J. S.; Eng, J. K.; Stein, S. E.; Aebersold, R. Building Consensus Spectral Libraries for Peptide Identification in Proteomics. *Nat Methods* **2008**, *5* (10), 873–875. <https://doi.org/10.1038/nmeth.1254>.
- (36) Craig, R.; Cortens, J. C.; Fenyo, D.; Beavis, R. C. Using Annotated Peptide Mass Spectrum Libraries for Protein Identification. *J. Proteome Res.* **2006**, *5* (8), 1843–1849.  
<https://doi.org/10.1021/pr0602085>.



- 1  
2  
3  
4  
5  
6  
7  
8  
9  
10  
11  
12  
13  
14  
15  
16  
17  
18  
19  
20  
21  
22  
23  
24  
25  
26  
27  
28  
29  
30  
31  
32  
33  
34  
35  
36  
37  
38  
39  
40  
41  
42  
43  
44  
45  
46  
47  
48  
49  
50  
51  
52  
53  
54  
55  
56  
57  
58  
59  
60
- (37) Frewen, B. E.; Merrihew, G. E.; Wu, C. C.; Noble, W. S.; MacCoss, M. J. Analysis of Peptide MS/MS Spectra from Large-Scale Proteomics Experiments Using Spectrum Libraries. *Anal. Chem.* **2006**, *78* (16), 5678–5684. <https://doi.org/10.1021/ac060279n>.
- (38) Huber, F.; Verhoeven, S.; Meijer, C.; Spreeuw, H.; Castilla, E.; Geng, C.; Van Der Hooft, J.; Rogers, S.; Belloum, A.; Diblen, F.; Spaaks, J. Matchms - Processing and Similarity Evaluation of Mass Spectrometry Data. *JOSS* **2020**, *5* (52), 2411. <https://doi.org/10.21105/joss.02411>.
- (39) Remoroza, C. A.; Burke, M. C.; Yang, X.; Sheetlin, S.; Mirokhin, Y.; Markey, S. P.; Tchekhovskoi, D. V.; Stein, S. E. Mass Spectral Library Methods for Analysis of Site-Specific N-Glycosylation: Application to Human Milk Proteins. *J. Proteome Res.* **2022**, *21* (10), 2421–2434. <https://doi.org/10.1021/acs.jproteome.2c00286>.
- (40) Schmid, R.; Heuckeroth, S.; Korf, A.; Smirnov, A.; Myers, O.; Dyrland, T. S.; Bushuiev, R.; Murray, K. J.; Hoffmann, N.; Lu, M.; Sarvepalli, A.; Zhang, Z.; Fleischauer, M.; Dührkop, K.; Wesner, M.; Hoogstra, S. J.; Rudt, E.; Mokshyna, O.; Brungs, C.; Ponomarov, K.; Mutabdzija, L.; Damiani, T.; Pudney, C. J.; Earll, M.; Helmer, P. O.; Fallon, T. R.; Schulze, T.; Rivas-Ubach, A.; Bilbao, A.; Richter, H.; Nothias, L.-F.; Wang, M.; Orešič, M.; Weng, J.-K.; Böcker, S.; Jeibmann, A.; Hayen, H.; Karst, U.; Dorrestein, P. C.; Petras, D.; Du, X.; Pluskal, T. Integrative Analysis of Multimodal Mass Spectrometry Data in MZmine 3. *Nat Biotechnol* **2023**, *41* (4), 447–449. <https://doi.org/10.1038/s41587-023-01690-2>.
- (41) *Eidhammer I, Flikka K, Martens L, Mikalsen S-O (2007) Spectral Comparisons. Computational Methods for Mass Spectrometry pro Teomics. John Wiley & Sons, Ltd., West Sussex, Pp 159–178.*
- (42) Huber, F.; Ridder, L.; Verhoeven, S.; Spaaks, J. H.; Diblen, F.; Rogers, S.; Van Der Hooft, J. J. J. Spec2Vec: Improved Mass Spectral Similarity Scoring through Learning of Structural Relationships. *PLoS Comput Biol* **2021**, *17* (2), e1008724. <https://doi.org/10.1371/journal.pcbi.1008724>.
- (43) Huber, F.; Van Der Burg, S.; Van Der Hooft, J. J. J.; Ridder, L. MS2DeepScore: A Novel Deep Learning Similarity Measure to Compare Tandem Mass Spectra. *J Cheminform* **2021**, *13* (1), 84. <https://doi.org/10.1186/s13321-021-00558-4>.
- (44) Bittremieux, W.; Schmid, R.; Huber, F.; Van Der Hooft, J. J. J.; Wang, M.; Dorrestein, P. C. Comparison of Cosine, Modified Cosine, and Neutral Loss Based Spectrum Alignment For Discovery of Structurally Related Molecules. *J. Am. Soc. Mass Spectrom.* **2022**, *33* (9), 1733–1744. <https://doi.org/10.1021/jasms.2c00153>.
- (45) Moorthy, A. S.; Kearsley, A. J. Pattern Similarity Measures Applied to Mass Spectra. In *Progress in Industrial Mathematics: Success Stories*; Cruz, M., Parés, C., Quintela, P., Eds.; SEMA SIMAI Springer Series; Springer International Publishing: Cham, 2021; Vol. 5, pp 43–53. [https://doi.org/10.1007/978-3-030-61844-5\\_4](https://doi.org/10.1007/978-3-030-61844-5_4).
- (46) Konermann, L.; Ahadi, E.; Rodriguez, A. D.; Vahidi, S. Unraveling the Mechanism of Electrospray Ionization. *Anal. Chem.* **2013**, *85* (1), 2–9. <https://doi.org/10.1021/ac302789c>.
- (47) Karas, M.; Bahr, U.; Dülcks, T. Nano-Electrospray Ionization Mass Spectrometry: Addressing Analytical Problems beyond Routine. *Fresenius' Journal of Analytical Chemistry* **2000**, *366* (6–7), 669–676. <https://doi.org/10.1007/s002160051561>.
- (48) Kulyk, D. S.; Swiner, D. J.; Sahraeian, T.; Badu-Tawiah, A. K. Direct Mass Spectrometry Analysis of Complex Mixtures by Nanoelectrospray with Simultaneous Atmospheric



- Pressure Chemical Ionization and Electrophoretic Separation Capabilities. *Anal. Chem.* **2019**, *91* (18), 11562–11568. <https://doi.org/10.1021/acs.analchem.9b01456>.
- (49) Qiao, L.; Sartor, R.; Gasilova, N.; Lu, Y.; Tobolkina, E.; Liu, B.; Girault, H. H. Electrostatic-Spray Ionization Mass Spectrometry. *Anal. Chem.* **2012**, *84* (17), 7422–7430. <https://doi.org/10.1021/ac301332k>.
- (50) Damon, D. E.; Davis, K. M.; Moreira, C. R.; Capone, P.; Cruttenden, R.; Badu-Tawiah, A. K. Direct Biofluid Analysis Using Hydrophobic Paper Spray Mass Spectrometry. *Anal. Chem.* **2016**, *88* (3), 1878–1884. <https://doi.org/10.1021/acs.analchem.5b04278>.
- (51) Jiang, Y.; Cole, R. B. Oligosaccharide Analysis Using Anion Attachment in Negative Mode Electrospray Mass Spectrometry. *J. Am. Soc. Mass Spectrom.* **2005**, *16* (1), 60–70. <https://doi.org/10.1016/j.jasms.2004.09.006>.
- (52) Guan, B.; Cole, R. B. MALDI Linear-Field Reflectron TOF Post-Source Decay Analysis of Underivatized Oligosaccharides: Determination of Glycosidic Linkages and Anomeric Configurations Using Anion Attachment. *J. Am. Soc. Mass Spectrom.* **2008**, *19* (8), 1119–1131. <https://doi.org/10.1016/j.jasms.2008.05.003>.
- (53) Vinueza, N. R.; Gallardo, V. A.; Klimek, J. F.; Carpita, N. C.; Kenttämä, H. I. Analysis of Carbohydrates by Atmospheric Pressure Chloride Anion Attachment Tandem Mass Spectrometry. *Fuel* **2013**, *105*, 235–246. <https://doi.org/10.1016/j.fuel.2012.08.012>.
- (54) Amoah, E.; Acharya, S. R.; Seth, A.; Badu-Tawiah, A. K. Liquid Chromatography-Mass Spectrometry Approach for Characterizing Sucrose Isomers in Complex Mono-Floral Honey. *Anal Bioanal Chem* **2025**, *417* (20), 4709–4722. <https://doi.org/10.1007/s00216-025-05988-9>.
- (55) Gillet, L. C.; Navarro, P.; Tate, S.; Röst, H.; Selevsek, N.; Reiter, L.; Bonner, R.; Aebersold, R. Targeted Data Extraction of the MS/MS Spectra Generated by Data-Independent Acquisition: A New Concept for Consistent and Accurate Proteome Analysis. *Molecular & Cellular Proteomics* **2012**, *11* (6), O111.016717. <https://doi.org/10.1074/mcp.O111.016717>.
- (56) Ma, B.; Chen, J.; Zheng, H.; Fang, T.; Ogotu, C.; Li, S.; Han, Y.; Wu, B. Comparative Assessment of Sugar and Malic Acid Composition in Cultivated and Wild Apples. *Food Chemistry* **2015**, *172*, 86–91. <https://doi.org/10.1016/j.foodchem.2014.09.032>.
- (57) Li, M.; Du, J.; Zhang, K. Profiling of Carbohydrates in Commercial Beers and Their Influence on Beer Quality. *J Sci Food Agric* **2020**, *100* (7), 3062–3070. <https://doi.org/10.1002/jsfa.10337>.

1  
2  
3  
4  
5  
6  
7  
8  
9  
10  
11  
12  
13  
14  
15  
16  
17  
18  
19  
20  
21  
22  
23  
24  
25  
26  
27  
28  
29  
30  
31  
32  
33  
34  
35  
36  
37  
38  
39  
40  
41  
42  
43  
44  
45  
46  
47  
48  
49  
50  
51  
52  
53  
54  
55  
56  
57  
58  
59  
60

Open Access Article. Published on 30 April 2025. Downloaded on 5/1/2025 10:24:52 AM.  
This article is licensed under a Creative Commons Attribution-NonCommercial 3.0 Unported Licence.



The data that support the findings of this study are available in the supporting information of this article.

Analyst Accepted Manuscript

1  
2  
3  
4  
5  
6  
7  
8  
9  
10  
11  
12  
13  
14  
15  
16  
17  
18  
19  
20  
21  
22  
23  
24  
25  
26  
27  
28  
29  
30  
31  
32  
33  
34  
35  
36  
37  
38  
39  
40  
41  
42  
43  
44  
45  
46  
47  
48  
49  
50  
51  
52  
53  
54  
55  
56  
57  
58  
59  
60

Open Access Article. Published on 30 April 2022. Downloaded on 5/1/2022 10:24:52 AM.  
This article is licensed under a Creative Commons Attribution-NonCommercial 3.0 Unported Licence.

